Measurements of the absolute branching fractions of $B^+ \to X_{c\bar{c}}K^+$ and $B^+ \to \bar{D}^{(*)0}\pi^+$ at Belle

Y. Kato,[53] T. Iijima,[53,52] I. Adachi,[15,11] H. Aihara,[79] S. Al Said,[72,35] D. M. Asner,[63] V. Aulchenko,[3,61] T. Aushev,[51] R. Ayad,[72] V. Babu,[73] I. Badhrees,[72,34] A. M. Bakich,[71] V. Bansal,[63] E. Barberio,[48] P. Behera,[21] V. Bhardwaj,[18] B. Bhuyan,[20] J. Biswal,[30] A. Bozek,[58] M. Bračko,[46,30] T. E. Browder,[14] D. Červenkov,[4] P. Chang,[57] R. Cheaib,[26] V. Chekelian,[47] A. Chen,[55] B. G. Cheon,[13] K. Chilikin,[41,50] K. Cho,[36] S.-K. Choi,[12] Y. Choi,[70] D. Cinabro,[84] T. Czank,[77] N. Dash,[19] S. Di Carlo,[84] Z. Doležal,[4] Z. Drásal,[4] D. Dutta,[73] S. Eidelman,[3,61] D. Epifanov,[3,61] J. E. Fast,[63] T. Ferber,[7] B. G. Fulsom,[63] V. Gaur,[83] N. Gabyshev,[3,61] A. Garmash,[3,61] M. Gelb,[32] P. Goldenzweig,[32] D. Greenwald,[75] E. Guido,[28] J. Haba,[15,11] K. Hayasaka,[60] H. Hayashii,[54] M. T. Hedges,[14] S. Hirose,[52] W.-S. Hou,[57] K. Inami,[52] G. Inguglia,[7] A. Ishikawa,[77] R. Itoh,[15,11] M. Iwasaki,[62] Y. Iwasaki,[15] W. W. Jacobs,[22] I. Jaegle,[8] H. B. Jeon,[39] Y. Jin,[79] K. K. Joo,[5] T. Julius,[48] A. B. Kaliyar,[21] K. H. Kang,[39] G. Karyan,[7] T. Kawasaki,[60] H. Kichimi,[15] C. Kiesling,[47] D. Y. Kim,[68] J. B. Kim,[37] S. H. Kim,[13] Y. J. Kim,[36] K. Kinoshita,[6] P. Kodyš,[4] S. Korpar,[46,30] D. Kotchetkov,[14] P. Križan,[42,30] R. Kroeger,[26] P. Krokovny,[3,61] T. Kuhr,[43] R. Kulasiri,[33] A. Kuzmin,[3,61] Y.-J. Kwon,[86] J. S. Lange,[9] I. S. Lee,[13] C. H. Li,[48] L. Li,[66] L. Li Gioi,[47] J. Libby,[21] D. Liventsev,[83,15] M. Lubej,[30] T. Luo,[64] M. Masuda,[78] T. Matsuda,[49] M. Merola,[27] K. Miyabayashi,[54] H. Miyata,[60] R. Mizuk,[41,50,51] G. B. Mohanty,[73] H. K. Moon,[37] T. Mori,[52] R. Mussa,[28] E. Nakano,[62] M. Nakao,[15,11] T. Nanut,[30] K. J. Nath,[20] Z. Natkaniec,[58] M. Nayak,[84,15] M. Niiyama,[38] N. K. Nisar,[64] S. Nishida,[15,11] S. Ogawa,[76] S. Okuno,[31] H. Ono,[59,60] P. Pakhlov,[41,50] G. Pakhlova,[41,51] B. Pal,[6] C.-S. Park,[86] C. W. Park,[70] H. Park,[39] S. Paul,[75] T. K. Pedlar,[44] R. Pestotnik,[30] L. E. Piilonen,[83] M. Ritter,[43] A. Rostomyan,[7] Y. Sakai,[15,11] M. Salehi,[45,43] S. Sandilya,[6] Y. Sato,[52] V. Savinov,[64] O. Schneider,[40] G. Schnell,[1,17] C. Schwanda,[24] A. J. Schwartz,[6] Y. Seino,[60] K. Senyo,[85] M. E. Sevior,[48] V. Shebalin,[3,61] C. P. Shen,[2] T.-A. Shibata,[80] J.-G. Shiu,[57] F. Simon,[47,74] A. Sokolov,[25] E. Solovieva,[41,51] M. Starič,[30] J. F. Strube,[63] M. Sumihama,[10] K. Sumisawa,[15,11] T. Sumiyoshi,[81] M. Takizawa,[67,16,65] U. Tamponi,[28,82] K. Tanida,[29] F. Tenchini,[48] K. Trabelsi,[15,11] M. Uchida,[80] S. Uehara,[15,11] T. Uglov,[41,51] Y. Unno,[13] S. Uno,[15,11] P. Urquijo,[48] Y. Usov,[3,61] C. Van Hulse,[1] G. Varner,[14] K. E. Varvell,[71] V. Vorobyev,[3,61] C. H. Wang,[56] M.-Z. Wang,[57] P. Wang,[23] M. Watanabe,[60] S. Watanuki,[77] E. Widmann,[69] E. Won,[37] Y. Yamashita,[59] H. Ye,[7] J. Yelton,[8] C. Z. Yuan,[23] Y. Yusa,[60] Z. P. Zhang,[66] V. Zhilich,[3,61] V. Zhukova,[41,50] V. Zhulanov,[3,61] and A. Zupanc[42,30]

(The Belle Collaboration)

[1]*University of the Basque Country UPV/EHU, 48080 Bilbao*
[2]*Beihang University, Beijing 100191*
[3]*Budker Institute of Nuclear Physics SB RAS, Novosibirsk 630090*
[4]*Faculty of Mathematics and Physics, Charles University, 121 16 Prague*
[5]*Chonnam National University, Kwangju 660-701*
[6]*University of Cincinnati, Cincinnati, Ohio 45221*
[7]*Deutsches Elektronen–Synchrotron, 22607 Hamburg*
[8]*University of Florida, Gainesville, Florida 32611*
[9]*Justus-Liebig-Universität Gießen, 35392 Gießen*
[10]*Gifu University, Gifu 501-1193*
[11]*SOKENDAI (The Graduate University for Advanced Studies), Hayama 240-0193*
[12]*Gyeongsang National University, Chinju 660-701*
[13]*Hanyang University, Seoul 133-791*
[14]*University of Hawaii, Honolulu, Hawaii 96822*
[15]*High Energy Accelerator Research Organization (KEK), Tsukuba 305-0801*
[16]*J-PARC Branch, KEK Theory Center, High Energy Accelerator Research Organization (KEK), Tsukuba 305-0801*
[17]*IKERBASQUE, Basque Foundation for Science, 48013 Bilbao*
[18]*Indian Institute of Science Education and Research Mohali, SAS Nagar, 140306*
[19]*Indian Institute of Technology Bhubaneswar, Satya Nagar 751007*
[20]*Indian Institute of Technology Guwahati, Assam 781039*
[21]*Indian Institute of Technology Madras, Chennai 600036*
[22]*Indiana University, Bloomington, Indiana 47408*
[23]*Institute of High Energy Physics, Chinese Academy of Sciences, Beijing 100049*

[24]Institute of High Energy Physics, Vienna 1050
[25]Institute for High Energy Physics, Protvino 142281
[26]University of Mississippi, University, Mississippi 38677
[27]INFN—Sezione di Napoli, 80126 Napoli
[28]INFN—Sezione di Torino, 10125 Torino
[29]Advanced Science Research Center, Japan Atomic Energy Agency, Naka 319-1195
[30]J. Stefan Institute, 1000 Ljubljana
[31]Kanagawa University, Yokohama 221-8686
[32]Institut für Experimentelle Kernphysik, Karlsruher Institut für Technologie, 76131 Karlsruhe
[33]Kennesaw State University, Kennesaw, Georgia 30144
[34]King Abdulaziz City for Science and Technology, Riyadh 11442
[35]Department of Physics, Faculty of Science, King Abdulaziz University, Jeddah 21589
[36]Korea Institute of Science and Technology Information, Daejeon 305-806
[37]Korea University, Seoul 136-713
[38]Kyoto University, Kyoto 606-8502
[39]Kyungpook National University, Daegu 702-701
[40]École Polytechnique Fédérale de Lausanne (EPFL), Lausanne 1015
[41]P.N. Lebedev Physical Institute of the Russian Academy of Sciences, Moscow 119991
[42]Faculty of Mathematics and Physics, University of Ljubljana, 1000 Ljubljana
[43]Ludwig Maximilians University, 80539 Munich
[44]Luther College, Decorah, Iowa 52101
[45]University of Malaya, 50603 Kuala Lumpur
[46]University of Maribor, 2000 Maribor
[47]Max-Planck-Institut für Physik, 80805 München
[48]School of Physics, University of Melbourne, Victoria 3010
[49]University of Miyazaki, Miyazaki 889-2192
[50]Moscow Physical Engineering Institute, Moscow 115409
[51]Moscow Institute of Physics and Technology, Moscow Region 141700
[52]Graduate School of Science, Nagoya University, Nagoya 464-8602
[53]Kobayashi-Maskawa Institute, Nagoya University, Nagoya 464-8602
[54]Nara Women's University, Nara 630-8506
[55]National Central University, Chung-li 32054
[56]National United University, Miao Li 36003
[57]Department of Physics, National Taiwan University, Taipei 10617
[58]H. Niewodniczanski Institute of Nuclear Physics, Krakow 31-342
[59]Nippon Dental University, Niigata 951-8580
[60]Niigata University, Niigata 950-2181
[61]Novosibirsk State University, Novosibirsk 630090
[62]Osaka City University, Osaka 558-8585
[63]Pacific Northwest National Laboratory, Richland, Washington 99352
[64]University of Pittsburgh, Pittsburgh, Pennsylvania 15260
[65]Theoretical Research Division, Nishina Center, RIKEN, Saitama 351-0198
[66]University of Science and Technology of China, Hefei 230026
[67]Showa Pharmaceutical University, Tokyo 194-8543
[68]Soongsil University, Seoul 156-743
[69]Stefan Meyer Institute for Subatomic Physics, Vienna 1090
[70]Sungkyunkwan University, Suwon 440-746
[71]School of Physics, University of Sydney, New South Wales 2006
[72]Department of Physics, Faculty of Science, University of Tabuk, Tabuk 71451
[73]Tata Institute of Fundamental Research, Mumbai 400005
[74]Excellence Cluster Universe, Technische Universität München, 85748 Garching
[75]Department of Physics, Technische Universität München, 85748 Garching
[76]Toho University, Funabashi 274-8510
[77]Department of Physics, Tohoku University, Sendai 980-8578
[78]Earthquake Research Institute, University of Tokyo, Tokyo 113-0032
[79]Department of Physics, University of Tokyo, Tokyo 113-0033
[80]Tokyo Institute of Technology, Tokyo 152-8550
[81]Tokyo Metropolitan University, Tokyo 192-0397
[82]University of Torino, 10124 Torino

[83]*Virginia Polytechnic Institute and State University, Blacksburg, Virginia 24061*
[84]*Wayne State University, Detroit, Michigan 48202*
[85]*Yamagata University, Yamagata 990-8560*
[86]*Yonsei University, Seoul 120-749*

(Received 18 September 2017; published 25 January 2018)

We present the measurement of the absolute branching fractions of $B^+ \to X_{c\bar{c}}K^+$ and $B^+ \to \bar{D}^{(*)0}\pi^+$ decays, using a data sample of 772×10^6 $B\bar{B}$ pairs collected at the $\Upsilon(4S)$ resonance with the Belle detector at the KEKB asymmetric-energy e^+e^- collider. Here, $X_{c\bar{c}}$ denotes η_c, J/ψ, χ_{c0}, χ_{c1}, $\eta_c(2S)$, $\psi(2S)$, $\psi(3770)$, $X(3872)$, and $X(3915)$. We do not observe significant signals for $X(3872)$ or $X(3915)$ and set the 90% confidence level upper limits at $\mathcal{B}(B^+ \to X(3872)K^+) < 2.6 \times 10^{-4}$ and $\mathcal{B}(B^+ \to X(3915)K^+) < 2.8 \times 10^{-4}$. These represent the most stringent upper limit for $\mathcal{B}(B^+ \to X(3872)K^+)$ to date and the first limit for $\mathcal{B}(B^+ \to X(3915)K^+)$. The measured branching fractions for η_c and $\eta_c(2S)$ are the most precise to date, $\mathcal{B}(B^+ \to \eta_c K^+) = (12.0 \pm 0.8 \pm 0.7) \times 10^{-4}$ and $\mathcal{B}(B^+ \to \eta_c(2S)K^+) = (4.8 \pm 1.1 \pm 0.3) \times 10^{-4}$, where the first and second uncertainties are statistical and systematic, respectively.

DOI: 10.1103/PhysRevD.97.012005

I. INTRODUCTION

The discovery of the $X(3872)$ by the Belle Collaboration [1] opened a new era in the field of hadron spectroscopy. The $X(3872)$ does not correspond to any of the predicted charmonium states in the quark model [2], and is an exotic hadron candidate. The most natural interpretation of $X(3872)$ is a D^0 and $\bar{D}^{*0}$ molecular state, as its mass is quite close to the combined mass of these charmed mesons and it has $J^{PC} = 1^{++}$ [3], which is consistent with an S-wave $D^0\bar{D}^{*0}$ molecule state. However, a pure molecular interpretation cannot explain the large cross section observed by the CDF experiment in $p\bar{p}$ collisions at $\sqrt{s} = 1.9$ TeV [4]. Therefore, the most plausible explanation of $X(3872)$ is an admixture of a molecular state and a pure charmonium $\chi_{c1}(2P)$ [5]. The large value of the ratio $\mathcal{B}(X(3872) \to \psi(2S)\gamma)/\mathcal{B}(X(3872) \to J/\psi\gamma)$ [6,7] and the lack of observation of $\chi_{c1}(2P) \to \chi_{c1}\pi^+\pi^-$ [8] also support this interpretation. In order to understand the nature of $X(3872)$, a measurement of the absolute branching fraction $\mathcal{B}(B^+ \to X(3872)K^+)$ is quite useful [9]. With this measurement in hand, we can determine $\mathcal{B}(X(3872) \to f)$, where f is a possible final state, since the product of $\mathcal{B}(B^+ \to X(3872)K^+)$ and $\mathcal{B}(X(3872) \to f)$ is measured [10]. The measurement of $\mathcal{B}(B^+ \to X(3872)K^+)$ is possible in B-factory experiments operating at a center-of-mass energy that corresponds to the mass of the $\Upsilon(4S)$ resonance, where the $\Upsilon(4S)$ almost exclusively decays into a $B\bar{B}$ pair. Therefore, by exclusively reconstructing one B meson and identifying the K^+ in the decay of the other B meson, the missing mass technique can be used to reconstruct the $X(3872)$. In the past, *BABAR* used a similar approach to perform this measurement with an data set of 231.8×10^6 $B\bar{B}$ pairs, which resulted in an upper limit at 90% confidence level (C.L) of $\mathcal{B}(B^+ \to X(3872)K^+) < 3.2 \times 10^{-4}$ [11]. The Belle Collaboration measured the $\mathcal{B}(B^+ \to X(3872)K^+) \times \mathcal{B}(X(3872) \to D^0\bar{D}^0\pi^0)$ to be $(1.02 \pm 0.31^{0.21}_{0.29}) \times 10^{-4}$. This value provides the lower limit of the $\mathcal{B}(B^+ \to X(3872)K^+)$ as $\mathcal{B}(X(3872) \to D^0\bar{D}^0\pi^0)$ is smaller than unity. In this paper, we present a measurement of $\mathcal{B}(B^+ \to X(3872)K^+)$ using the full data sample of the Belle experiment, along with a simultaneous measurement of the various charmonium(-like) states ($X_{c\bar{c}}$) that appear in the missing mass spectrum. We measure the branching fractions of nine states: η_c, J/ψ, χ_{c0}, χ_{c1}, $\eta_c(2S)$, $\psi(2S)$, $\psi(3770)$, $X(3872)$, and $X(3915)$. In particular, the measurements of $\mathcal{B}(B^+ \to \eta_c K^+)$ and $\mathcal{B}(B^+ \to \eta_c(2S)K^+)$ are important. Past measurements of these values [11] limited the precision of the determination of the absolute branching fractions of η_c and $\eta_c(2S)$ [10]. Also, this is the first limit for $\mathcal{B}(B^+ \to X(3915)K^+)$. Finally, we present the measurement of $\mathcal{B}(B^+ \to \bar{D}^{(*)0}\pi^+)$, using a similar technique, where the $\bar{D}^{(*)0}$ is reconstructed from the missing mass. These are useful normalization modes for other B-meson decays such as $B^+ \to \bar{D}^{(*)0}K^+$ and $B^+ \to \bar{D}^{(*)0}\pi^+\pi^+\pi^-$.

The remaining sections of the paper are organized as follows: in Sec. II, the Belle detector and the data samples used are described. In Sec. III, an overview of the analysis method is provided. In Sec. IV, the analysis approach for the $B^+ \to \bar{D}^{(*)0}\pi^+$ decay is described. In Sec. V, the $B^+ \to X_{c\bar{c}}K^+$ analysis is presented. In Sec. VI, the relevant systematic uncertainties are discussed. Finally, in Sec. VII, the conclusion of this paper is presented.

II. DATA SAMPLES AND THE BELLE DETECTOR

We use a data sample of 772×10^6 $B\bar{B}$ pairs recorded with the Belle detector at the KEKB asymmetric-energy e^+e^- collider [12]. The Belle detector is a large-solid-angle magnetic spectrometer that consists of a silicon vertex detector (SVD), a 50-layer central drift chamber (CDC), an array of aerogel threshold Cherenkov counters (ACC), a barrel-like arrangement of time-of-flight scintillation counters (TOF), and an electromagnetic calorimeter comprised of CsI(Tl) crystals (ECL) located inside a superconducting solenoid coil that provides a 1.5 T magnetic field. An iron flux-return located outside of the coil is instrumented to detect K_L^0 mesons and to identify muons. The Belle detector is described in detail elsewhere [13].

We use Monte-Carlo (MC) simulated events generated using `EvtGen` [14] and `JETSET` [15] that include QED final-state radiation [16]. The events are then processed by a detector simulation based on `GEANT3` [17]. We produce signal MC events to obtain the reconstruction efficiency and the mass resolution for signal events. We also use background MC samples to study the missing-mass distribution in the background process $\Upsilon(4S) \to B\bar{B}$ and $e^+e^- \to q\bar{q}$ ($q = u$, d, s, c and b) with statistics 6 times that of data.

III. ANALYSIS OVERVIEW

In this analysis, we fully reconstruct one of the two charged B mesons ($B_{\rm tag}$) via hadronic states and require at least one charged kaon or pion candidate among the charged particles not used for the $B_{\rm tag}$ reconstruction. The kaon or pion, coming from the other charged B meson, $B_{\rm sig}$, is required to have a charge opposite that of $B_{\rm tag}$. The $B_{\rm tag}$ is reconstructed in one of 1104 hadronic decays using a hierarchical hadronic full reconstruction algorithm based on the NeuroBayes neural-network package [18]. The quality of a $B_{\rm tag}$ candidate is represented by a single NeuroBayes output-variable classifier ($O_{\rm NB}$), which includes event-shape information to suppress continuum events. We require $O_{\rm NB}$ to be greater than 0.01, which retains 90% of true $B_{\rm tag}$ candidates and rejects 70% of fake $B_{\rm tag}$ candidates. The beam constrained mass $M_{\rm bc} = \sqrt{E^{*2}_{\rm beam}/c^4 - |\vec{p}^{*2}_{\rm tag}|/c^2}$, where $E^*_{\rm beam}$ and $\vec{p}^*_{\rm tag}$ are the beam-energy and the reconstructed $B_{\rm tag}$ three-momenta, respectively, in the center-of-mass frame, is required to be greater than 5.273 GeV$/c^2$.

About 18% of the events contain multiple $B_{\rm tag}$ candidates that pass all the selection criteria. In such an event, the $B_{\rm tag}$ with the greatest $O_{\rm NB}$ is retained. The $B_{\rm tag}$ reconstruction efficiency is roughly 0.3%. Figure 1 shows the $M_{\rm bc}$ distribution for data with the $O_{\rm NB}$ requirement applied. The selections of the charged kaon and pion daughters of $B_{\rm sig}$ are performed based on vertex information from the tracking system (SVD and CDC) and

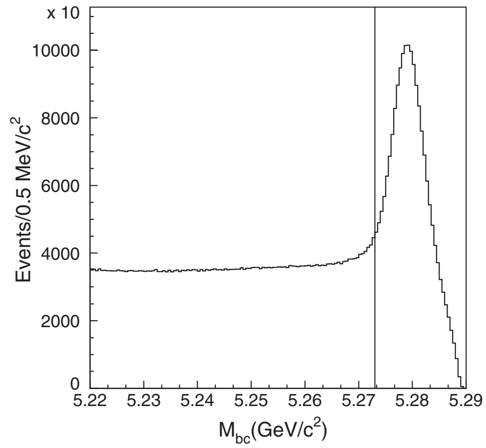

FIG. 1. $M_{\rm bc}$ distribution for data after the requirement on the $O_{\rm NB}$. Vertical line shows the lower bound of the selection criteria.

likelihood values $\mathcal{L}_K$ and $\mathcal{L}_\pi$ provided by the hadron identification system, ionization loss in the CDC, the number of detected Cherenkov photons in the ACC, and the time-of-flight measured by the TOF [19]. A charged track is required to have a point of closest approach to the interaction point that is within 5.0 cm along the z axis and 0.40 cm in the transverse (r-ϕ) plane. The z axis is opposite the positron beam direction. A track is identified as a kaon (pion) if the likelihood ratio $\mathcal{L}(K\!:\!\pi)$ ($\mathcal{L}(\pi\!:\!K)$) is greater than 0.6. The likelihood ratio is defined as $\mathcal{L}(i\!:\!j) = \mathcal{L}_i/(\mathcal{L}_i + \mathcal{L}_j)$. The efficiencies of hadron identification are about 90% for both pions and kaons. The momentum-averaged probability to misidentify a pion (kaon) track as a kaon (pion) track is about 9% (10%). We identify the signal as a peak at the nominal $X_{c\bar{c}}$ or $\bar{D}^{*0}$ mass in the distribution of missing mass,

$$M_{\rm miss(h)} = \sqrt{(p^*_{\rm e^+e^-} - p^*_{\rm tag} - p^*_{\rm h})^2}/c, \qquad (1)$$

where $M_{\rm miss(h)}$ is the missing mass recoiling against the hadron h (π^+ or K^+), and $p^*_{e^+e^-}$, $p^*_{\rm tag}$, and p^*_h are the four-momenta of the electron-positron initial state, $B_{\rm tag}$, and h, respectively, in the center-of-mass frame. The probability to observe multiple kaon or pion candidates in the $M_{{\rm miss}(h)}$ range of interest (2.6 GeV$/c^2 < M_{{\rm miss}(K^+)} <$ 4.1 GeV$/c^2$ and $M_{{\rm miss}(\pi^+)} <$ 2.5 GeV$/c^2$) in an event is 2.8% and 0.3%, respectively. We do not apply a best-candidate selection if multiple candidates are found.

The beam-energy resolution is a dominant contribution to the $M_{\rm bc}$ resolution, and event-by-event fluctuations of $M_{\rm bc}$ from the nominal B meson mass are directly correlated to the event-by-event fluctuation of the beam energy. We apply a correction to account for the event-by-event fluctuation of the beam energy using a linear relation to $M_{\rm bc}$. The corrected beam-energy improves the missing mass resolution by 8%, 4%, and 2% for $X(3872)$, J/ψ, and

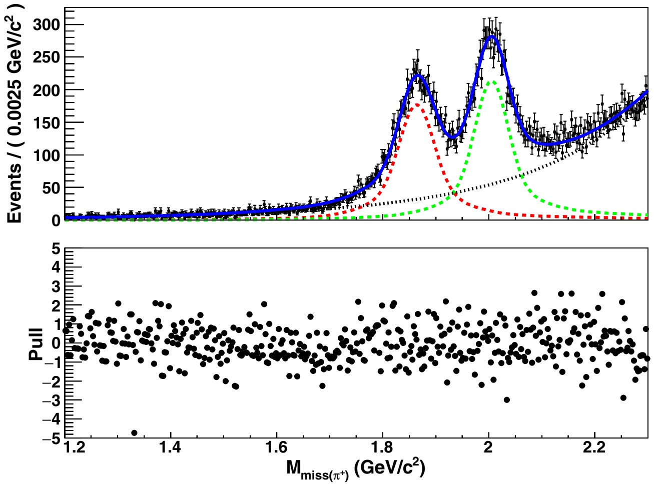

FIG. 2. Observed $M_{\mathrm{miss}(\pi^+)}$ distribution. Points with error bars represent data. The solid, dashed, and dotted lines represent the total fit result, the contribution from $\bar{D}^0$ and $\bar{D}^{*0}$, and the contribution from the background, respectively.

D^0, respectively. The validity of the beam-energy correction is checked using high-statistics samples $B^+ \to D^{(*)0}\pi^+$, $B^+ \to D^{(*)0}\pi^+\pi^+\pi^-$, and $B^+ \to J/\psi K^+$ samples. We divide the samples into two sets with M_{bc} smaller or larger than the nominal B^+ mass [10]. The peak positions in the $M_{\mathrm{miss}(h)}$ distribution for both data sets without the beam-energy correction are significantly different from their expected masses and are consistent within uncertainty after the correction. We blinded the missing mass distribution in the range 3.3 GeV$/c^2 < M_{\mathrm{miss}(K^+)} <$ 4.0 GeV$/c^2$ until the analysis procedure was fixed. Branching fractions are obtained using the following equations,

$$\mathcal{B} = \frac{N_{\mathrm{sig}}}{2N_{B^\pm}\epsilon}, \tag{2}$$

$$N_{B^\pm} = N_{\Upsilon(4S)}\mathcal{B}(\Upsilon(4S) \to B^+B^-), \tag{3}$$

where N_{sig} is the signal yield obtained from the fit to the missing mass distribution, ϵ is the reconstruction efficiency for B_{tag} and pion or kaon in B_{sig}, and $N_{\Upsilon(4S)}$ is the number of accumulated $\Upsilon(4S)$ events. We use a value of 0.514 for $\mathcal{B}(\Upsilon(4S) \to B^+B^-)$ [10]. The factor of two in Eq. (2) originates from the inclusion of the charge-conjugate mode.

IV. ANALYSIS OF $B^+ \to \bar{D}^{(*)0}\pi^+$ DECAY

Figure 2 shows the observed $M_{\mathrm{miss}(\pi^+)}$ distribution, where clear peaks corresponding to $\bar{D}^0$ and $\bar{D}^{*0}$ are visible. In order to extract the signal $\bar{D}^{(*)0}$ yields, a binned likelihood fit is performed. The probability density function (PDF) for the signal peak is the sum of three Gaussian functions based on a study of large simulated samples of signal decays. The mean value for one Gaussian function is allowed to differ from that of the other two to accommodate for the tail in high-mass regions resulting from B_{tag} decays with photons. The relative weights of the three Gaussian functions are fixed to the values obtained from the signal MC. We introduce two parameters: the global offset of the mean $(\mu_{\mathrm{data}} - \mu_{\mathrm{MC}})$ and the global resolution scale factor $(\sigma_{\mathrm{data}}/\sigma_{\mathrm{MC}})$ to accommodate for a possible difference in the shape in the signal MC and data. The PDF for background events is represented by a second-order exponential: $\exp(ax + bx^2)$, where a and b are free parameters in the fit. The validity of using this function as a background PDF is confirmed by fitting to the background MC and sideband data, which is defined within the region 5.22 GeV$/c^2 < M_{\mathrm{bc}} <$ 5.26 GeV$/c^2$. The fit returns a reasonable χ^2/ndf, where ndf is number of degree of freedom. χ^2 is not improved by increasing the exponential order. The mass range above 2.3 GeV$/c^2$ is not included in the fit to avoid contributions from excited D mesons.

Table I summarizes the branching fraction measurements for $B^+ \to \pi^+\bar{D}^{(*)0}$. The values of $(\mu_{\mathrm{data}} - \mu_{\mathrm{MC}})$ and $(\sigma_{\mathrm{data}}/\sigma_{\mathrm{MC}})$ are found to be quite consistent at 0 MeV$/c^2$ and 1, respectively, indicating that the signal MC describes the signal shape well. The measured branching fractions are consistent with the world averages [10] within 1.1σ taking into account the fact that almost all past measurements assumed $\mathcal{B}(\Upsilon(4S) \to B^+B^-) = 0.5$.

V. ANALYSIS OF $B^+ \to X_{c\bar{c}}K^+$ DECAY

Figure 3 shows the observed and fitted $M_{\mathrm{miss}(K^+)}$ distributions. We again perform a binned likelihood fit to extract the signal $X_{c\bar{c}}$ yields. In the analysis of the high-statistics sample of $B^+ \to \bar{D}^{(*)0}\pi^+$, we confirm that the signal shape is consistent between data and MC. Therefore, we fix the signal PDF to be the histogram PDF from signal MC generated with the mass and natural width of the $X_{c\bar{c}}$ states fixed to the world averages [10]. We consider nine $X_{c\bar{c}}$ in the fit: η_c, J/ψ, χ_{c0}, χ_{c1}, $\eta_c(2S)$, $\psi(2S)$, $\psi(3770)$,

TABLE I. Summary of the branching fraction measurements for $B^+ \to \bar{D}^{(*)0}\pi^+$ decays. The first uncertainties for the branching fractions are statistical and the second are systematic.

Mode	N_{sig}	$(\mu_{\mathrm{data}} - \mu_{\mathrm{MC}})$ (MeV$/c^2$)	$(\sigma_{\mathrm{data}}/\sigma_{\mathrm{MC}})$	ϵ (10^{-3})	$\mathcal{B}$ (10^{-3})	World average for $\mathcal{B}$ (10^{-3}) [10]
$B^+ \to \pi^+\bar{D}^0$	8550 ± 190	-0.5 ± 0.8	0.994 ± 0.025	2.48 ± 0.02	$4.34 \pm 0.10 \pm 0.25$	4.80 ± 0.15
$B^+ \to \pi^+\bar{D}^{*0}$	9980 ± 250	-0.8 ± 0.8	1.035 ± 0.029	2.61 ± 0.02	$4.82 \pm 0.12 \pm 0.35$	5.18 ± 0.26

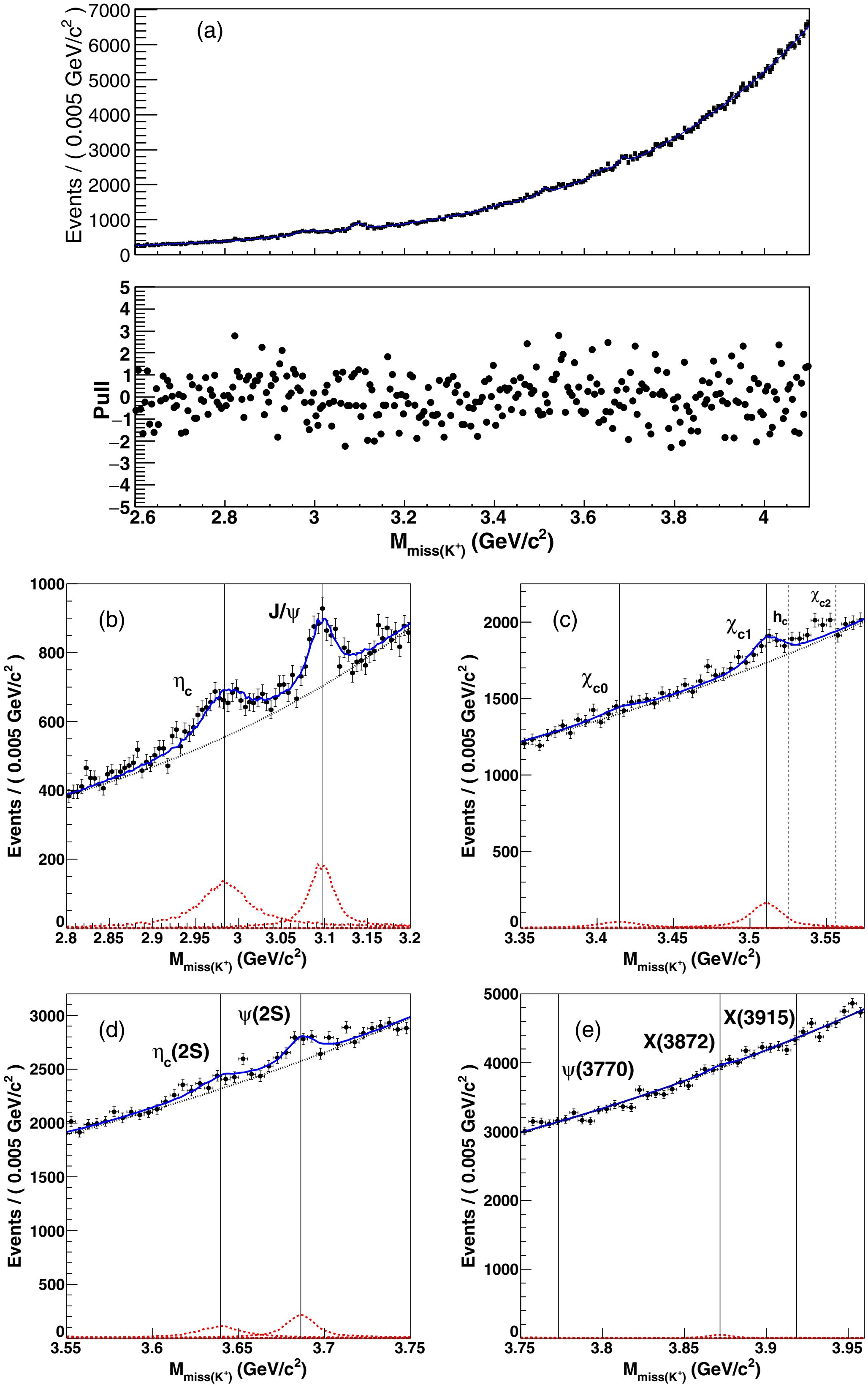

FIG. 3. Observed $M_{\mathrm{miss}(K^+)}$ distributions:(a) shows the full $M_{\mathrm{miss}(K^+)}$ region, with pull distribution, and (b), (c), (d), and (e) are for zoomed plots for specific $X_{c\bar{c}}$. Points with error bars represent data. Vertical solid lines show the nominal mass of $X_{c\bar{c}}$ included in the fit. Vertical dashed lines show the ones not included in the fit. Solid line represents the total fit result. Dashed and dotted lines are $X_{c\bar{c}}$ contributions and background contributions, respectively.

TABLE II. Summary of the branching fraction measurements for $B^+ \to X_{c\bar{c}} K^+$ decay. For the branching fractions, the first uncertainties are statistical and the second are systematic. Values in brackets for $\mathcal{B}$ represent the 90% C.L. upper limits.

Mode	Yield	Significance (σ)	$\epsilon(10^{-3})$	$\mathcal{B}$ (10^{-4})	World average for $\mathcal{B}$ (10^{-4}) [10]
η_c	2590 ± 180	14.2	2.73 ± 0.02	$12.0 \pm 0.8 \pm 0.7$	9.6 ± 1.1
J/ψ	1860 ± 140	13.7	2.65 ± 0.02	$8.9 \pm 0.6 \pm 0.5$	10.26 ± 0.031
χ_{c0}	430 ± 190	2.2	2.67 ± 0.02	$2.0 \pm 0.9 \pm 0.1$ (<3.3)	$1.50^{+0.15}_{-0.14}$
χ_{c1}	1230 ± 180	6.8	2.68 ± 0.02	$5.8 \pm 0.9 \pm 0.5$	4.79 ± 0.23
$\eta_c(2S)$	1050 ± 240	4.1	2.77 ± 0.02	$4.8 \pm 1.1 \pm 0.3$	3.4 ± 1.8
$\psi(2S)$	1410 ± 210	6.6	2.79 ± 0.02	$6.4 \pm 1.0 \pm 0.4$	6.26 ± 0.24
$\psi(3770)$	-40 ± 310	-	2.76 ± 0.02	$-0.2 \pm 1.4 \pm 0.0$ (<2.3)	4.9 ± 1.3
$X(3872)$	260 ± 230	1.1	2.79 ± 0.01	$1.2 \pm 1.1 \pm 0.1$ (<2.6)	(<3.2)
$X(3915)$	80 ± 350	0.3	2.79 ± 0.01	$0.4 \pm 1.6 \pm 0.0$ (<2.8)	-

$X(3872)$, and $X(3915)$. We do not include h_c and χ_{c2} because their branching fractions are measured to be very small [10]: $\mathcal{B}(B^+ \to K^+ h_c) < 3.8 \times 10^{-5}$ at 90% C.L. and $\mathcal{B}(B^+ \to K^+ \chi_{c2}) = (1.1 \pm 0.4) \times 10^{-5}$. The background PDF is a second-order exponential, as for $B^+ \to \pi^+ \bar{D}^{(*)0}$, and is again validated with background MC and the data sideband. The statistical significance of each $X_{c\bar{c}}$ state is determined from the log-likelihood ratio $-2\ln(\mathcal{L}_0/\mathcal{L})$, where $\mathcal{L}_0$ ($\mathcal{L}$) is the likelihood for the fit without (with) the signal component. When we evaluate the significance for a $X_{c\bar{c}}$ state, the other $X_{c\bar{c}}$ states are included in the fit. The branching fractions are determined using Eq. (2). For χ_{c0}, $\psi(3770)$, and $X(3872)$, the significances are smaller than three standard deviations (σ). We also set 90% C.L. upper limit for branching fractions to these states using the CLs technique [20].

The results are summarized in Table II. The upper limit for $\mathcal{B}(B^+ \to X(3872)K^+)$ is the most stringent to date. The upper limit for the $\mathcal{B}(B^+ \to X(3915)K^+)$ is determined for the first time. The measurements for $\mathcal{B}(B^+ \to \eta_c K^+)$ and $\mathcal{B}(B^+ \to \eta_c(2S)K^+)$ are the most precise to date. In particular, this is the first significant measurement of $\mathcal{B}(B^+ \to \eta_c(2S)K^+)$. For $\mathcal{B}(B^+ \to \psi(3770)K^+)$, we do not see a significant signal and the measured value is smaller than world average by 2.7σ. For the other measurements, the values are consistent with world averages within 1.7σ.

In Fig. 3(c), we see an enhancement near 3545 MeV$/c^2$, where no known charmonium state exists. We attempt to fit this by including an additional contribution using signal MC PDF with a mass of 3545 MeV$/c^2$ and a natural width of 0 MeV. An offset for the peak position is introduced as a free parameter. The signal yield is 738 ± 189 events at the peak position of 3544.2 ± 2.8 MeV$/c^2$, which is 4.3σ lower than the mass of the χ_{c2}. The $-2\ln(\mathcal{L}_0/\mathcal{L})$ value is 16.5. Since the signal region is very wide compared to the experimental resolution, we estimate the probability to observe such an enhancement in a single experiment. We perform one million pseudoexperiments in which background events are generated with the same shape and yield as data. Multiple fits, each including signal with a natural width of zero and a mass value incremented by 1 MeV/c^2 across the fit range for successive fits, are performed and the highest $-2\ln(\mathcal{L}_0/\mathcal{L})$ in one pseudoexperiment is retained. The probability to observe an enhancement with $-2\ln(\mathcal{L}_0/\mathcal{L})$ greater than 16.5 is 0.43%, which corresponds to a global significance of 2.8σ. We, therefore, conclude that the enhancement is not significant.

VI. SYSTEMATIC UNCERTAINTY

A summary of the systematic uncertainties for each $X_{c\bar{c}}$ and $\bar{D}^{(*)0}$ state is provided in Table III. We consider the following systematic uncertainties for the branching fraction measurements. The systematic uncertainty for the efficiency of the charged hadron identification is estimated from the yield of $D^{*+} \to D^0\pi^+$, $D^0 \to K^-\pi^+$ with and without the hadron identification requirements. We apply a correction factor to the particle identification efficiencies based on the ratio of the efficiencies found in the MC and data samples. The uncertainty of the correction factor is treated as the systematic uncertainty. The systematic uncertainty due to the charged track reconstruction efficiency is estimated using the decay chain $D^{*+} \to \pi^+ D^0$, $D^0 \to \pi^+\pi^- K^0_S$, and $K^0_S \to \pi^+\pi^-$ where $K^0_S \to \pi^+\pi^-$ is either partially or fully reconstructed. The ratio between the yields of partially and fully reconstructed signals are compared between data and MC; the difference of 0.35% per track is taken as the systematic uncertainty. The systematic uncertainty from the reconstruction efficiency of $B_{\rm tag}$ is estimated using a hadronic-tag analysis in which $B_{\rm sig}$ decays to $D^{(*)}\ell\nu$, where l is electron or muon [21]. The yield for this signal is compared between data and MC, and the difference is implemented as a correction factor for each $B_{\rm tag}$ decay mode. The averaged correction factor used in this analysis is 0.76 independent of $X_{c\bar{c}}$. The signal and background efficiencies are multiplied by this factor. The main origin of the correction factor is understood to result from the fact that branching fractions for some of the $B_{\rm tag}$ decays in the MC generation are outdated and inconsistent withe the most recent measurements. Furthermore, this correction factor is also determined in the $B^- \to \tau^-\nu$

TABLE III. Summary of the systematic uncertainties (%).

Source	η_c	J/ψ	χ_{c0}	χ_{c1}	$\eta_c(2S)$	$\psi(2S)$	$\psi(3770)$	$X(3872)$	$X(3915)$	$\bar{D}^0$	$\bar{D}^{*0}$
PID	0.8	0.8	0.7	0.7	0.8	0.7	0.8	0.9	0.9	0.9	0.9
Tracking	0.35	0.35	0.35	0.35	0.35	0.35	0.35	0.35	0.35	0.35	0.35
B_{tag}	4.6	4.6	4.6	4.6	4.6	4.6	4.6	4.6	4.6	4.6	4.6
$\mathcal{B}(\Upsilon(4S))$	1.2	1.2	1.2	1.2	1.2	1.2	1.2	1.2	1.2	1.2	1.2
$N_{\Upsilon(4S)}$	1.4	1.4	1.4	1.4	1.4	1.4	1.4	1.4	1.4	1.4	1.4
M & Γ (PDG)	1.5	0.4	1.6	0.2	0.8	0.4	0.4	0.1	5.7	-	-
Fit bias	0.0	0.2	1.9	0.6	0.4	1.0	0.7	0.6	1.6	0.2	0.2
$\mu_{\mathrm{data}} - \mu_{\mathrm{MC}}$ and $\sigma_{\mathrm{data}}/\sigma_{\mathrm{MC}}$	0.3	1.5	0.8	3.6	1.0	3.7	1.7	3.4	2.0	-	-
Histogram PDF	0.7	0.5	3.2	1.5	2.4	1.5	2.5	0.9	2.4	-	-
Decay simulation	2.1	3.0	1.1	2.0	1.3	1.0	0.0	0.9	0.5	-	-
Background parametrization	0.6	0.3	1.7	0.6	3.8	0.2	2.0	1.8	3.5	2.8	5.0
χ_{c2}/h_c	0.0	0.0	1.3	3.9	0.7	0.6	1.1	0.4	2.5	-	-
Signal MC statistics	0.8	0.8	0.8	0.8	0.8	0.8	0.8	0.4	0.8	0.8	0.8
Total	5.8	6.1	7.0	7.8	7.1	6.7	6.4	6.5	9.5	5.8	7.2

analysis independently using sideband region of extra ECL energy [22]. The correction factor is found to be consistent with that obtained from $D^{(*)}\ell\nu$, which indicates that it is generally independent of the B_{sig} decay mode. The uncertainty of this correction factor, 4.6%, is regarded as the systematic uncertainty. Note that the correction for lepton identification efficiency and associated systematic uncertainty were not taken into account in Ref. [21]. These are implemented in this analysis. The world average of $\mathcal{B}(\Upsilon(4S) \to B^+B^-)$ is $(51.4 \pm 0.6)\%$ [10], which corresponds to a systematic uncertainty of 1.2%. The systematic uncertainty for the $N_{\Upsilon(4S)}$ is assigned as 1.4%. The systematic uncertainty due to the mass and width of each state is estimated by performing fits while varying the mass and width by the world-average uncertainties [10]. The systematic uncertainty on the fitter bias is estimated by performing pseudoexperiments. We generate pseudodata from the background and signal shapes determined from the background MC and the signal MC, respectively. The background yields are taken from the sideband of data defined as $M_{\mathrm{miss}(K^+)} < 3.3\ \mathrm{GeV}/c^2$ or $M_{\mathrm{miss}(K^+)} > 4.0\ \mathrm{GeV}/c^2$, and signal yields are determined from the world averages of the branching fractions and the reconstruction efficiencies. We perform a binned likelihood fit to extract the signal yields in each pseudoexperiment. The difference between the mean of the extracted signal yields and the input mass value is taken as the systematic uncertainty. The systematic uncertainty due to the $B^+ \to X_{c\bar{c}}K^+$ signal PDF arises from uncertainties of $\mu_{\mathrm{data}} - \mu_{\mathrm{MC}}$ and $\sigma_{\mathrm{data}}/\sigma_{\mathrm{MC}}$ in the $B^+ \to D^{0(*)}\pi^+$ fit. This is evaluated by performing a fit with the PDF shape parameters changed within their uncertainties after averaging the result for $\bar{D}^0$ and $\bar{D}^{*0}$. All the charmonium states are changed simultaneously in this case. The systematic uncertainty arising from the finite statistics of the signal MC is estimated by repeatedly modifying the histogram-PDF bin contents within the Poisson uncertainty and then refitting. The root mean square of the extracted signal yield distribution is regarded as the systematic uncertainty.

The reconstruction efficiency of the B_{tag} may depend on the decay of $X_{c\bar{c}}$ states. As our knowledge of the decay modes of each $X_{c\bar{c}}$ is limited, a systematic uncertainty is assigned in the following way. For each $X_{c\bar{c}}$ except $\psi(3770)$, the sum of the known branching fractions is not equal to 100%. In the default estimation of the branching fraction, unknown decay modes are filled with decays into $u\bar{u}$, $d\bar{d}$, and $s\bar{s}$, that hadronize via PYTHIA. The systematic uncertainty is estimated by eliminating the PYTHIA-generated decay and taking the difference with the nominal efficiency. For $X(3872)$ and $X(3915)$, the PYTHIA decay is not implemented by default. Therefore, the systematic uncertainty is estimated by implementing the PYTHIA decay with a branching fraction of 50%. The systematic uncertainty on the background assumption is estimated by performing a fit after changing the order of the exponential background's polynomial exponent from quadratic to cubic. We perform a fit including h_c and χ_{c2} with yields fixed to their world averages and upper limit for the branching fractions, respectively. The difference of the yields from the default fit is regarded as a systematic uncertainty. The statistical uncertainty of the signal reconstruction efficiency due to signal MC statistics is regarded as systematic uncertainty.

VII. CONCLUSION

We present the measurement of the absolute branching fractions for $B^+ \to X_{c\bar{c}}K^+$, where $X_{c\bar{c}}$ denotes η_c, J/ψ, χ_{c0}, χ_{c1}, $\eta_c(2S)$, $\psi(2S)$, $\psi(3770)$, $X(3872)$, and $X(3915)$, and also $B^+ \to \pi^+D^{(*)0}$. We do not observe a significant signal for $X(3872)$ and set an 90% C.L. upper limit of

$\mathcal{B}(B^+ \to X(3872)K^+) < 2.6 \times 10^{-4}$, which is more stringent than the one determined by *BABAR* [11] (3.2×10^{-4}). The lower limit of $\mathcal{B}(X(3872) \to f)$ is based on *BABAR*'s measurement. Our result improves these lower limits. We set the 90% C.L. upper limit of $\mathcal{B}(B^+ \to X(3915)K^+) < 2.8 \times 10^{-4}$ for the first time.

We measure $\mathcal{B}(B^+ \to \eta_c K^+) = (12.0 \pm 0.8 \pm 0.7) \times 10^{-4}$ and $\mathcal{B}(B^+ \to \eta_c(2S)K^+) = (4.8 \pm 1.1 \pm 0.3) \times 10^{-4}$, which are the most accurate measurements to date. In particular, this is the first significant measurement for $\mathcal{B}(B^+ \to \eta_c(2S)K^+)$. The current world average of $\mathcal{B}(\eta_c(2S) \to K\bar{K}\pi)$ is $(1.9 \pm 0.4 \pm 1.1)\%$ [10], where the second uncertainty is dominated by the measurement of $\mathcal{B}(B^+ \to \eta_c(2S)K^+) = (3.4 \pm 1.8) \times 10^{-4}$ by *BABAR* [11]. Our measurement significantly improves the precision of $\mathcal{B}(\eta_c(2S) \to K\bar{K}\pi)$. In addition, this measurement can contribute to many other decays involving the $\eta_c(2S)$ such as $\psi(2S) \to \gamma\eta_c(2S)$ by BESIII [23] and $\eta_c(2S) \to p\bar{p}$ by LHCb [24]. Finally, we measure $\mathcal{B}(B^+ \to \bar{D}^0\pi^+) = (4.34 \pm 0.10 \pm 0.25) \times 10^{-3}$ and $\mathcal{B}(B^+ \to \bar{D}^{*0}\pi^+) = (4.82 \pm 0.12 \pm 0.35) \times 10^{-3}$, which are consistent with the world averages [10]. The latter is the most precise measurement from a single experiment.

ACKNOWLEDGMENTS

We thank the KEKB group for the excellent operation of the accelerator; the KEK cryogenics group for the efficient operation of the solenoid; and the KEK computer group, the National Institute of Informatics, and the Pacific Northwest National Laboratory (PNNL) Environmental Molecular Sciences Laboratory (EMSL) computing group for valuable computing and Science Information NETwork 5 (SINET5) network support. We acknowledge support from the Ministry of Education, Culture, Sports, Science, and Technology (MEXT) of Japan, the Japan Society for the Promotion of Science (JSPS), and the Tau-Lepton Physics Research Center of Nagoya University; the Australian Research Council; Austrian Science Fund under Grant No. P 26794-N20; the National Natural Science Foundation of China under Contracts No. 11435013, No. 11475187, No. 11521505, No. 11575017, No. 11675166, No. 11705209; Key Research Program of Frontier Sciences, Chinese Academy of Sciences (CAS), Grant No. QYZDJ-SSW-SLH011; the CAS Center for Excellence in Particle Physics (CCEPP); Fudan University Grant No. JIH5913023, No. IDH5913011/003, No. JIH5913024, No. IDH5913011/002; the Ministry of Education, Youth and Sports of the Czech Republic under Contract No. LTT17020; the Carl Zeiss Foundation, the Deutsche Forschungsgemeinschaft, the Excellence Cluster Universe, and the VolkswagenStiftung; the Department of Science and Technology of India; the Istituto Nazionale di Fisica Nucleare of Italy; National Research Foundation (NRF) of Korea Grants No. 2014R1A2A2A01005286, No. 2015R1A2A2A01003280, No. 2015H1A2A1033649, No. 2016R1D1A1B01010135, No. 2016K1A3A7A09005 603, No. 2016R1D1A1B02012900; Radiation Science Research Institute, Foreign Large-size Research Facility Application Supporting project and the Global Science Experimental Data Hub Center of the Korea Institute of Science and Technology Information; the Polish Ministry of Science and Higher Education and the National Science Center; the Ministry of Education and Science of the Russian Federation and the Russian Foundation for Basic Research; the Slovenian Research Agency; Ikerbasque, Basque Foundation for Science and Ministry of Economy and Competitiveness (MINECO) (Juan de la Cierva), Spain; the Swiss National Science Foundation; the Ministry of Education and the Ministry of Science and Technology of Taiwan; and the United States Department of Energy and the National Science Foundation. This work is supported by a Grant-in-Aid for Scientific Research (S) "Probing New Physics with Tau-Lepton" (No. 26220706), and Grant-in-Aid for Scientific Research on Innovative Areas "Elucidation of New Hadrons with a Variety of Flavors".

[1] S. K. Choi *et al.* (Belle Collaboration), Phys. Rev. Lett. **91**, 262001 (2003).

[2] S. L. Olsen, Int. J. Mod. Phys. A **20**, 240 (2005).

[3] R. Aaij *et al.* (LHCb Collaboration), Phys. Rev. Lett. **110**, 222001 (2013).

[4] A. Abulencia *et al.* (CDF Collaboration), Phys. Rev. Lett. **98**, 132002 (2007).

[5] M. Takizawa and S. Takeuchi, Prog. Theor. Exp. Phys. **2013**, 903D01 (2013).

[6] R. Aaij *et al.* (LHCb Collaboration), Nucl. Phys. **B886**, 665 (2014).

[7] B. Aubert *et al.* (*BABAR* Collaboration), Phys. Rev. Lett. **102**, 132001 (2009).

[8] V. Bhardwaj *et al.* (Belle Collaboration), Phys. Rev. D **93**, 052016 (2016).

[9] C. M. Zanetti, M. Nielsen, and R. D. Matheus, Phys. Lett. B **702**, 359 (2011).

[10] C. Patrignani *et al.* (Particle Data Group Collaboration), Chin. Phys. C **40**, 100001 (2016).

[11] B. Aubert *et al.* (*BABAR* Collaboration), Phys. Rev. Lett. **96**, 052002 (2006).

[12] S. Kurokawa and E. Kikutani, Nucl. Instrum. Methods Phys. Res., Sect. A **499**, 1 (2003), and other papers included in this volume; T. Abe *et al.*, Prog. Theor. Exp. Phys. **2013**, 03A001 and following articles up to 03A011 (2013).

[13] A. Abashian *et al.* (Belle Collaboration), Nucl. Instrum. Methods Phys. Res., Sect A **479**, 117 (2002); also see detector section in J. Brodzicka *et al.*, Prog. Theory. Exp. Phys. (2012) 04D001.

[14] D. J. Lange, Nucl. Instrum Methods Phys. Res., Sect. A **462**, 152 (2001).

[15] T. Sjøstrand, Comput. Phys. Commun. **82**, 74 (1994).

[16] E. Barberio and Z. Wąs, Comput. Phys. Commun. **79**, 291 (1994).

[17] R. Brun *et al.*, GEANT3.21, CERN Report No. DD/EE/84-1 (1984).

[18] M. Feindt, F. Keller, M. Kreps, T. Kuhr, S. Neubauer, D. Zander, and A. Zupanc, Nucl. Instrum. Methods Phys. Res., Sect. A **654**, 432 (2011).

[19] E. Nakano, Nucl. Instrum. Methods Phys. Res., Sect. A **494**, 402 (2002).

[20] A. L. Read, J. Phys. G **28**, 2693 (2002).

[21] A. Sibidanov *et al.* (Belle Collaboration), Phys. Rev. D **88**, 032005 (2013).

[22] I. Adachi *et al.* (Belle Collaboration), Phys. Rev. Lett. **110**, 131801 (2013).

[23] M. Ablikim *et al.* (BES Collaboration), Phys. Rev. Lett. **109**, 042003 (2012).

[24] R. Aaij *et al.* (LHCb Collaboration), Phys. Lett. B **769**, 305 (2017).